Quantum Chemical Study of the Acrolein (CH_2CHCHO) + OH + O_2 Reactions

Rubik Asatryan,[†] Gabriel da Silva,[‡] and Joseph W. Bozzelli*[,†]

Department of Chemistry and Environmental Science, New Jersey Institute of Technology, Newark, New Jersey 07102, USA, and Department of Chemical and Biomolecular Engineering, The University of Melbourne, Victoria 3010, Australia

Received: May 26, 2010; Revised Manuscript Received: July 5, 2010

Acrolein, a β-unsaturated (acrylic) aldehyde, is one of the simplest multifunctional molecules, containing both alkene and aldehyde groups. Acrolein is an atmospheric pollutant formed in the photochemical oxidation of the anthropogenic VOC 1,3-butadiene, and serves as a model compound for methacrolein (MACR) and methyl vinyl ketone (MVK), the major oxidation products of the biogenic VOC isoprene. In addition, acrolein is involved in combustion and biological oxidation processes. This study presents a comprehensive theoretical analysis of the acrolein + OH + O_2 addition reactions, which is a key photochemical oxidation sequence, using the G3SX and CBS-QB3 theoretical methods. Both ab initio protocols provide relatively similar results, although the CBS-QB3 method systematically under-predicts literature heats of formation using atomization enthalpies, and also provides lower transition state barrier heights. Several new low-energy pathways for unimolecular reaction of the acrolein−OH−O_2 radicals are identified, with energy at around or below that of the acrolein−OH isomers + O_2. In each case these novel reactions have the potential to reform the hydroxyl radical (OH) and form coproducts that include glyoxal, glycolaldehyde ($HOCH_2CHO$), formaldehyde (HCHO), CO, and substituted epoxides. Analogous reaction schemes are developed for the photochemical oxidation of MACR and MVK, producing a number of observed oxidation products. The reaction MACR + OH + O_2 → hydroxyacetone + OH + CO is expected to be of particular importance. This study also proposes that O_2 addition to chemically activated acrolein−OH adducts can provide prompt regeneration of OH in the atmospheric oxidation of acrolein, via a double activation mechanism. This mechanism can also be extended to isoprene, MVK, and MACR. The importance of the novel chemistry revealed here in the atmospheric oxidation of acrolein and other structurally related OVOCs and VOCs requires further investigation. Additionally, a critical evaluation of the acrolein heat of formation is presented, and a new value of −16.7 ± 1.0 kcal mol^{-1} is recommended along with other thermochemical properties, from a W1 level calculation.

Introduction

Acrolein, CH_2CHCHO, is a β-unsaturated acrylic aldehyde that plays an important role in atmospheric chemistry as an oxidation product of the anthropogenic pollutant butadiene.[1−5] Acryloylperoxy nitrate (APAN), $CH_2CHC(O)O_2NO_2$, has been observed in the urban atmosphere, with higher concentrations in regions with active petroleum industries.[3,4] This compound is a peroxyacetyl nitrate-like (PAN-like) compound formed from NO_2 reacting with the acrolein peroxy radical $CH_2CHC(O)OO^{\bullet}$, and its observation in urban plumes provides evidence for acrolein as an oxidation product of anthropogenic emissions. Acrolein can also be considered a surrogate or base compound for the carbonyls methacrolein (MACR) and methyl vinyl ketone (MVK) and is therefore a useful model compound in understanding their oxidation. MACR and MVK are the major photochemical oxidation products of isoprene,[6−8] the second most important volatile organic compound (VOC) in Earth's atmosphere (behind methane), and the key biogenic VOC controlling oxidation chemistry within the forested planetary boundary layer.[9] Acrolein is also a key oxygenated intermediate in hydrocarbon combustion, being involved in reactions of the allyl radical[10] and in kerosene oxidation.[11] Acrolein is a neurotoxic byproduct of lipid peroxidation, a process associated with oxidative stress and linked to Alzheimer's disease and other conditions.[12] Accordingly, it is important that we understand the oxidation chemistry of acrolein. In the atmosphere, as well as in combustion systems and biological media, oxidation initiated by the hydroxyl radical (OH) is a key process. The OH-initiated oxidation of acrolein has been investigated by a number of authors,[13,14] but it is not yet fully characterized.

Orlando and Tyndall[14] have shown in an environmental chamber experiment using FTIR spectroscopy that the main products of the acrolein + OH reaction in air are CO, CO_2, HCHO, and $HOCH_2CHO$ (glycolaldehyde). These authors determined that at room temperature around 68% of the acrolein + OH reaction takes place via H atom abstraction from the aldehyde group. The remainder of this reaction occurs via OH addition to the double bond, with 80% at the terminal β carbon and only 20% at the inner α C atom site, adjacent to the formyl group. The acrolein + OH reaction is therefore thought to result in the following initial products:

$$CH_2CHCHO + OH \rightarrow CH_2CHC^{\bullet}O + H_2O \ (68\%)$$

$$\rightarrow CH_2(OH)C^{\bullet}HCHO \ (26\%)$$

$$\rightarrow C^{\bullet}H_2CH(OH)CHO \ (6\%)$$

Several detailed theoretical studies exist on the initial reaction of acrolein with OH.[15−17] Olivella and Solé[15] studied this process

* To whom correspondence should be addressed. E-mail: bozzelli@njit.edu.
[†] New Jersey Institute of Technology.
[‡] The University of Melbourne.

10.1021/jp104828a
Published on Web 07/27/2010

using open-shell versions of QCISD(T) theory, considering each of the above three reactions. It was determined that acrolein and OH formed a prereaction complex with enthalpy below that of the reactants. From here, the barrier for H atom abstraction was found to be 1.1 kcal mol^{-1} below the reactant energies, with OH addition to the respective β and α carbons requiring barriers 0.7 kcal mol^{-1} below and 0.8 kcal mol^{-1} above the reactant energies (0 K). These results are qualitatively in agreement with experiment, as theory predicts that around 75% of the acrolein + OH reaction proceeds by H atom abstraction to form the $CH_2CHC^{\bullet}O$ radical. Vega-Rodriguez and Alvarez-Idaboy[16] also presented a theoretical study of the acrolein + OH reactions, which predicted that 57% of the reaction proceeded via abstraction.

Although the formation of these initial $CH_2CHC^{\bullet}O$, $C^{\bullet}H_2CH(OH)CHO$, and $CH_2(OH)C^{\bullet}HCHO$ radicals from the acrolein + OH reaction is now relatively well-understood, from both experiment and theory, there is less information on their further reaction with O_2. These oxygenated free radicals formed in acrolein oxidation are also sufficiently simple that they can be generated from other sources in reacting gas-phase systems, especially hydrocarbon and oxygenated hydrocarbon combustion, such as the oxidation of aldehydes, ethers, and esters.[18]

We have recently reported preliminary results on the reaction of acrolein and its $CH_2CHC^{\bullet}O$, $C^{\bullet}H_2CH(OH)CHO$, and $CH_2(OH)C^{\bullet}HCHO$ radicals with O_2, which can result in observed acrolein oxidation products such as glycolaldehyde as well as a variety of cyclic oxygenated molecules.[19] Here, we present a detailed theoretical study of the association of acrolein with OH, with particular emphasis on O_2 addition to the resultant $C_3H_5O_2$ radical species. This work reveals several new low-energy pathways expected to play an important role in atmospheric oxidation and combustion processes. A mechanism is also proposed for prompt product formation upon OH addition to acrolein in air, which includes regeneration of an OH radical that is consumed in this process.

Computational Methods

Cross sections of the $C_3H_5O_4$ energy surface relevant to acrolein oxidation are studied using the G3SX[20] and CBS-QB3[21] model chemistries, in Gaussian 03[22] and Gaussian 09.[23] The G3SX method uses B3LYP/6-31G(2df,p) optimized structures, vibrational frequencies, and zero point energies in a series of single-point wave function theory energy calculations from HF through MP2, MP3/MP4, and QCISD(T) theory, featuring basis sets of incrementally decreasing size. These energies are combined with the B3LYP zero-point energy and empirical scaling corrections to arrive at the final G3SX energy. The CBS-QB3 method is another composite theoretical protocol that uses B3LYP optimized structures and single-point wave function theory energies. CBS-QB3 theory is based on B3LYP/6-311G(2d,d,p) structures with an MP2 level energy extrapolated to the complete basis set limit, combined with further MP4 and CCSD(T) energies obtained with smaller basis sets, along with several other correction terms. In effect, both theoretical protocols attempt to approximate the QCISD(T)/CCSD(T) energy at the complete basis set limit, accounting for electron correlation and truncation of the one-electron basis set in a computationally efficient manner. Both G3SX and CBS-QB3 theory are broadly accurate for a range of thermochemical properties and barrier heights. The G3SX and CBS-QB3 methods reproduce all energies in the G2/97 test set with mean unsigned errors (MUEs) of 0.93 and 1.21 kcal mol^{-1}, respectively.[20] With the DBH24/08 database of representative reaction barrier heights, the G3SX and CBS-QB3 methods provide MUEs of 0.57 and 1.62 kcal mol^{-1}, respectively.[24]

Standard enthalpies of formation are obtained for all stationary points (minima and transition states) from atomization calculations, as described recently.[25] All structures reported are for the lowest-energy conformer located, where interconversion of conformers can be achieved via low energy internal rotations. Transition states are characterized as having only one negative eigenvalue of Hessian (force constant) matrices. For minima, the absence of an imaginary frequency verifies that structures are true minima at their respective levels of theory. The intrinsic reaction coordinate (IRC) procedure (as implemented in Gaussian 09) is used to identify the reactants and products connected to each transition state. For all reported stationary points we provide optimized structures and vibrational frequencies at the B3LYP/6-31G(2df,p) level and energies at the G3SX and CBS-QB3 levels, as Supporting Information.

Results and Discussion

This study is concerned with reactions of the two $C_3H_5O_4$ peroxy radicals that form from addition of OH and then O_2 to acrolein. Below, a discussion is provided on calculated enthalpies of formation reported in this study with the G3SX and CBS-QB3 theoretical methods. Following this, addition of OH to acrolein at the outer (terminal, β) and inner (internal, α) carbon atoms, followed by O_2 addition, is considered. Finally, the potential importance of these findings in acrolein oxidation, and atmospheric chemistry in general, is discussed.

Enthalpies of Formation. Standard enthalpies of formation ($\Delta_f H^\circ_{298}$, kcal mol^{-1}) for all minima and transition states in both OH/O_2 addition processes are listed in Table 1, calculated at the G3SX and CBS-QB3 levels. Agreement between the two methods is relatively good, with mean signed deviation of +2.19 kcal mol^{-1} and mean unsigned deviation of 2.22 kcal mol^{-1}; this indicates that the CBS-QB3 enthalpies of formation are consistently lower than those calculated with the G3SX method. This systematic deviation is heightened for the transition states, where the mean signed deviation is +3.41 kcal mol^{-1}, reflecting the improved performance of the G3SX method over CBS-QB3 at replicating barrier heights.[24] For the minima with known heats of formation,[26−34] the G3SX method reproduces these values with a MUE of 0.53 kcal mol^{-1}, MSE of only −0.01 kcal mol^{-1}, and maximum error of 0.90 kcal mol^{-1}, consistent with the known performance of this method.[20,24,25] The CBS-QB3 enthalpies of formation replicate the literature values with a MUE of 1.04 kcal mol^{-1}, MSE of +0.81 kcal mol^{-1}, and maximum error of 1.90 kcal mol^{-1}, again indicating a systematic underprediction of $\Delta_f H^\circ_{298}$. Furthermore, errors in the G3SX enthalpies (relative to experiment) are more tightly clustered than the CBS-QB3 enthalpies, with respective standard deviations of 0.63 and 0.92 kcal mol^{-1}. Despite (in fact, due to) the systematic nature of the deviations witnessed between the G3SX and CBS-QB3 atomization heats of formation, there is relatively little difference in reaction enthalpies relative to the reactants acrolein + OH + O_2. Here, the mean unsigned deviation is 1.05 kcal mol^{-1} (1.57 kcal mol^{-1} for the transition states alone), although all but one of the CBS-QB3 relative enthalpies are smaller than those calculated at the G3SX level. These results, when taken together, indicate that both methods can accurately reproduce reaction enthalpies, although CBS-QB3 enthalpies of formation calculated using atomization reactions are systematically low (whereas the G3SX method is consistently within "chemical accuracy"). Furthermore, the CBS-QB3 method appears to under-predict barrier heights, consistent with recent benchmark-

TABLE 1: Standard Enthalpies of Formation ($\Delta_f H°_{298}$) for All Minima and Transition States in the Acrolein + OH + O_2 Addition Mechanisms[a]

	$\Delta_f H°_{298}$ (kcal mol^{-1})		
	G3SX	CBS-QB3	Literature
CH_2CHCHO	–16.0	–15.6	-16.5 ± 2.4[26–28]
OH	9.2	8.8	8.91 ± 0.07[29]
$CH_2(OH)C^•HCHO$	–42.1	–43.4	
$C^•H_2CH(OH)CHO$	–34.5	–35.1	
O_2	0.9	–0.9	0
$CH_2(OH)CH(OO^•)CHO$	–65.5	–67.8	
$CH_2(O^•)CH(OOH)CHO$	–42.9	–46.7	
$CH_2(OH)CH(OOH)C^•O$	–62.3	–64.5	
$CH_2(OO^•)CH(OH)CHO$	–67.5	–69.7	
$CH_2(OOH)CH(O^•)CHO$	–46.6	–48.9	
$CH_2(OOH)CH(OH)C^•O$	–61.5	–64.0	
$CH_2(OOH)C^•(OH)CHO$	–75.4	–78.3	
HC(O)CHO	–51.6	–52.6	-50.7 ± 0.2[30]
HCHO	–26.5	–27.3	-26.05 ± 0.42[31]
$CH_2(OH)CHO$	–76.3	–77.4	-75.6 ± 0.8[32]
CO	–26.3	–26.9	-26.417 ± 0.041[33]
$CH_2(OOH)C^•HOH$	–31.1	–32.9	
$CH_2C(CHO)OH$	–63.1	–63.2	
HO_2	3.3	2.0	2.94 ± 0.06[34]
c-$CH_2OC(OH)(CHO)$-	–86.6	–88.5	
TSβ1	–43.0	–46.5	
TSβ2	–41.9	–44.7	
TSβ3	–45.4	–48.4	
TSβ4	–46.4	–53.5	
TSα1	–44.7	–48.5	
TSα2	–41.8	–44.0	
TSα3	–48.1	–50.9	
TSα4	–52.1	–54.5	
TSα5	–44.0	–47.1	
TSα6	–53.4	–56.2	
TSα7	–56.5	–60.5	

[a] Transition state numbering defined in Figures 1 and 4.

ing.[24] For TSβ4 the discrepancy between the two methods is especially large (5.3 kcal mol^{-1} relative to acrolein + OH + O_2), reflecting a recent result of ours on the *s*-triazine + OH reaction,[35] where it was suggested that the CBS-QB3 method (and not G3SX) failed to reproduce the actual barrier height.

Some discussion is warranted on the enthalpy of formation of acrolein. Despite being the most common C_3H_4O isomer, a reliable experimental value for the acrolein enthalpy of formation is not (to the best of our knowledge) available. The literature value of $\Delta_f H°_{298} = -16.5 \pm 2.4$ kcal mol^{-1} adopted in Table 1 was reported by Li and Baer[27] and is the average of three previous computational values.[28] Li and Baer also recommend $\Delta_f H°_0 = -13.9 \pm 2.4$ kcal mol^{-1}, with corresponding enthalpy content ($H°_{298} - H°_0$) of 3.32 kcal mol^{-1}. In the earlier literature, Alfassi and Benson[36] used group additivity to estimate $\Delta_f H°_{298} = -17.74$ kcal mol^{-1}; these authors also make reference to an unpublished experimental value of -17.79 kcal mol^{-1} cited by Anderson and Hood.[37] The critically evaluated data tables of Lias et al.[38] on the thermochemistry of gas-phase ions and their neutral parents report the acrolein heat of formation as -18 kcal mol^{-1}; the reference for this value,[39] however, estimates $\Delta_f H°_{298} = -20.6$ kcal mol^{-1} from group additivity considerations (the discrepancy possibly indicates correction to 0 K). A number of theoretical determinations of the acrolein heat of formation have also emerged since the work of Li and Baer.[27] Sebbar et al.[40] reported the acrolein heat of formation as -17.76 ± 0.41 kcal mol^{-1} from isodesmic calculations at the G3MP2B3 level, whereas similar B3LYP/6-311G(d,p) calculations provided a value of -18.65 ± 0.95 kcal mol^{-1}.[41] Kondo et al.[42] determined the acrolein heat of formation using the G2 (-15.9 kcal mol^{-1}) and G2MP2 methods (-15.9 kcal mol^{-1}), and with the atom additivity corrected methods AAC-G2 (-15.5 kcal mol^{-1}) and AAC-G2MP2 (-14.7 kcal mol^{-1}). Recently, Morales and Martínez[43] have suggested $\Delta_f H°_{298} = -15.08$ kcal mol^{-1} for acrolein, from CBS-Q level calculations on an atomization work reaction.

TABLE 2: Recommended Thermochemical Properties for Acrolein[a]

T (K)	$S°$ (cal mol^{-1} K^{-1})	C_p (cal mol^{-1} K^{-1})	$H°_T - H°_0$ (kcal mol^{-1})
298.15	66.72	16.47	3.39
300	66.82	16.55	3.42
400	72.11	20.28	5.27
500	76.99	23.51	7.46
600	81.52	26.19	9.95
800	89.64	30.26	15.62
1000	96.72	33.14	21.98
1500	111.07	37.35	39.74
2000	122.12	39.39	58.98

[a] $\Delta_f H°_{298} = -16.70 \pm 1.0$ kcal mol^{-1}.

It is apparent from the above survey that the acrolein enthalpy of formation likely lies in the range of -14 to -19 kcal mol^{-1}. To assist in refining the enthalpy of formation and other thermochemical properties of this important compound we have performed a benchmark-level W1 atomization calculation,[44] which is expected to provide heats of formation with 95% confidence interval uncertainties of around ± 1 kcal mol^{-1}. Thermochemical properties for acrolein are evaluated using B3LYP/cc-pVTZ+d structures, moments of inertia, and unscaled vibrational frequencies. Calculations of entropy and heat capacity treat rotation about the C−C bond as an unsymmetrical hindered internal rotor, from a relaxed B3LYP/cc-pVTZ+d level dihedral angle scan (5° intervals). The program lamm, within the MultiWell suite,[45] was used to evaluate moments of inertia and rotational constants as a function of dihedral angle. At the W1 level we determine $\Delta_f H°_{298} = -16.70 \pm 1.0$ kcal mol^{-1} and $\Delta_f H°_0 = -14.25 \pm 1.0$ kcal mol^{-1}, with $H°_{298} - H°_0 = 3.39$ kcal mol^{-1}. We feel that these values are presently the best available, although they provide little difference to those recommended by Li and Baer.[27] Other important thermochemical properties ($S°$, C_p, $H°_T$ - $H°_0$) are listed in Table 2, from 298.15 to 2000 K.

Outer (β) OH Addition. An energy diagram for acrolein oxidation initiated by OH addition to the β carbon atom is provided in Figure 1. Color-coding of the three reactants illustrates from where each of the O and H atoms in the different products originates, which may be useful in validating the proposed mechanisms in isotope labeled studies. Optimized structures for the $C_3H_5O_4$ radicals involved in this process are depicted in Figure 2, with transition state structures provide in Figure 3.

The initial OH addition reaction is exothermic by around 35 kcal mol^{-1}, whereas O_2 addition to the resultant $CH_2(OH)C^•HCHO$ radical is exothermic by a further 24 kcal mol^{-1}. The overall process is exothermic by 59.6 kcal mol^{-1} at the G3SX level of theory (60.1 kcal mol^{-1} at the CBS-QB3 level), and results in production of the $CH_2(OH)CH(OO^•)CHO$ peroxy radical. Typically, in atmospheric chemistry we only consider bimolecular reactions of peroxy radicals with species like NO, NO_2, HO_2, and RO_2. Abstraction of an O atom from $CH_2(OH)CH(OO^•)CHO$ by NO, forming the oxyl radical $CH_2(OH)CH(O^•)CHO$ (along with NO_2), is thought to ultimately

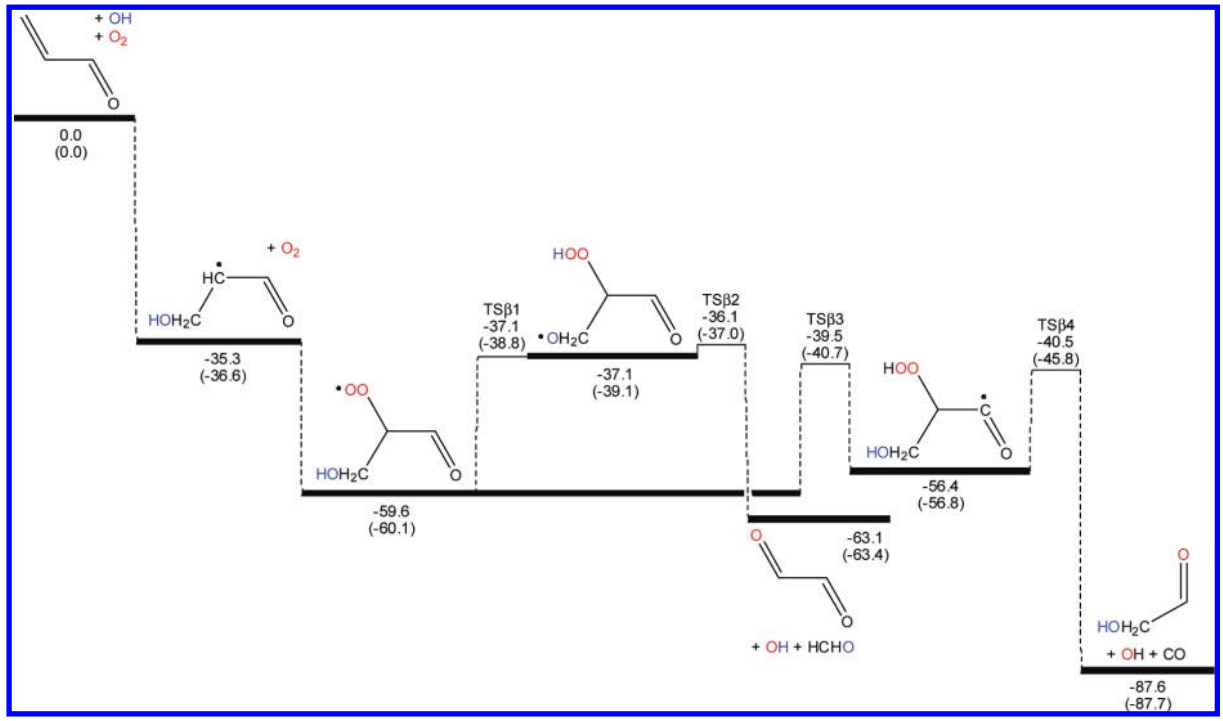

Figure 1. Energy surface for β OH addition to acrolein in air. Numbers are relative 298 K enthalpies with the G3SX (CBS-QB3) methods, in kcal mol^{-1}.

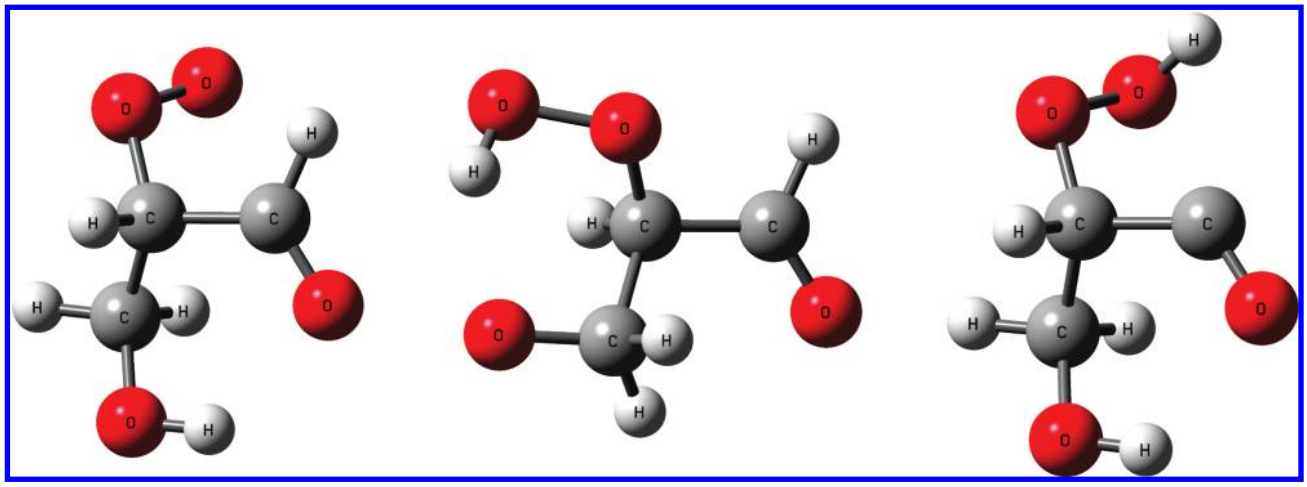

Figure 2. Optimized structures for $C_3H_5O_4$ minima arising from β OH addition to acrolein in air. Calculated at the B3LYP/6-31G(2df,p) level.

lead to glycolaldehyde (CH_2OHCHO) + CO + HO_2 and perhaps glyoxal (HC(O)CHO) + formaldehyde (HCHO) + HO_2. Experiments on the OH-initiated oxidation of acrolein detect glycolaldehyde, glyoxal, formaldehyde, and CO as products.[14]

The unimolecular decomposition of peroxy radicals formed in the photochemical oxidation of common VOCs and OVOCs at atmospheric conditions, given low levels of active radicals such as NO and HO_2 is emerging as a potentially important process.[46−48] Furthermore, unstable peroxy radicals like HC(O)C(OO•)O are thought to react via chemically activated radical + O_2 mechanisms.[49] The CH_2(OH)CH(OO•)CHO radical has both β-hydroxyperoxy and α-formylperoxy functionality, from which intramolecular H atom abstraction reactions may proceed with relatively low barriers,[46−49] making them of potential significance to atmospheric chemistry.

Figure 1 reveals that the CH_2(OH)CH(OO•)CHO radical formed from β OH addition to acrolein in air has several isomerization/decomposition pathways available with energy at around or even below that of CH_2(OH)C•HCHO + O_2. Intramolecular abstraction of H from the hydroxy group (via TSβ1) requires 22.5 kcal mol^{-1} at the G3SX level of theory, and produces an unstable oxyl radical intermediate, CH_2(O•)CH(OOH)CHO, that somewhat resembles a cyclic HCHO−OH−CH(O)CHO complex.[47] Dissociation of this unstable species produces the acrolein oxidation products glyoxal and formaldehyde, while also regenerating the initial OH radical consumed in the reaction scheme. The overall barrier for this decomposition mechanism is similar to that required for decomposition of the isoprene β-hydroxyperoxy radicals.[46,47] A lower-energy pathway is for intramolecular H atom abstraction from the α-formyl group (TSβ3), where the barrier is only 20.1 kcal mol^{-1} at the G3SX level (19.4 kcal mol^{-1} with CBS-QB3), or 4.2 kcal mol^{-1} below the CH_2(OH)C•HCHO + O_2 energy. This reaction produces the CH_2(OH)CH(OOH)C•O radical, which can further dissociate to glycolaldehyde + OH + CO with a barrier below that for formation of the radical (there is a significant difference between the G3SX and CBS-QB3 barrier heights for this reaction, but in either case CH_2(OH)CH(OOH)C•O is

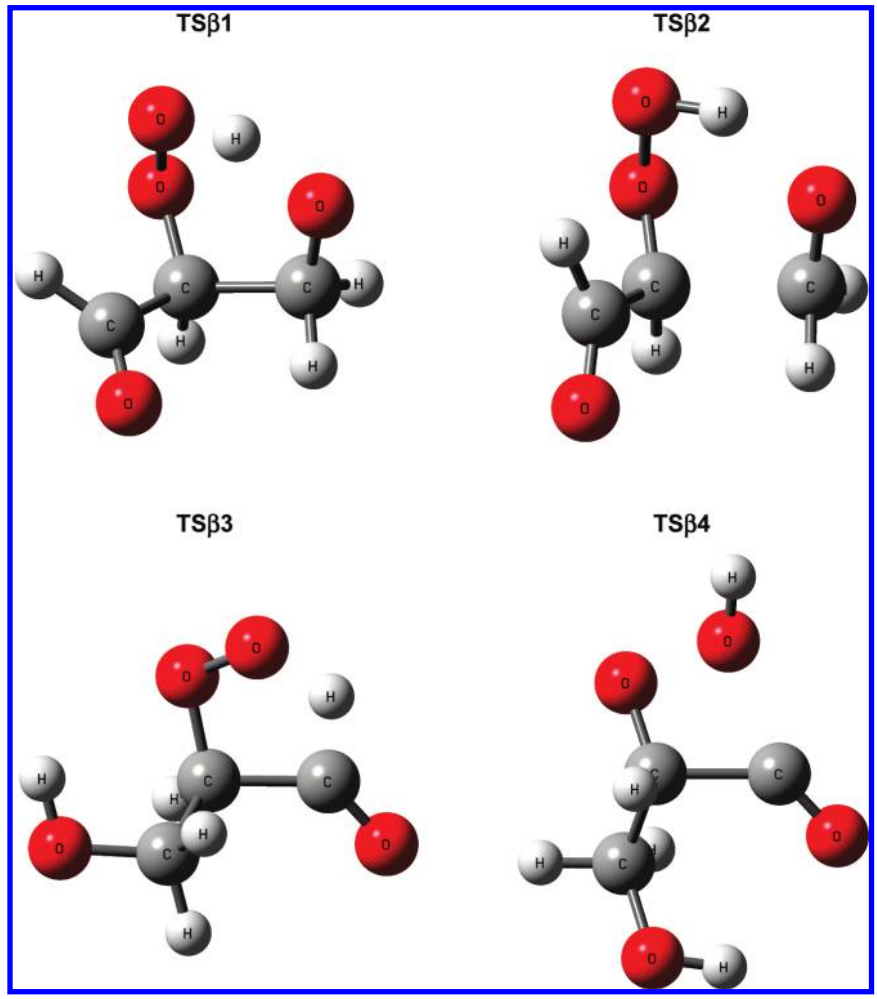

Figure 3. Optimized structures for $C_3H_5O_4$ transition states arising from β OH addition to acrolein in air. Calculated at the B3LYP/6-31G(2df,p) level.

expected to be unstable toward further decomposition). This process is analogous to that proposed for the HC(O)CO + O_2 reaction,[49] and also achieves the regeneration of OH.

The mechanism reported for β OH addition to acrolein in air provides pathways to several of the observed acrolein oxidation products, including glycolaldehyde and glyoxal. The limiting barrier heights for both decomposition processes are between 19 and 23 kcal mol^{-1}, which is in the range for which these unimolecular reactions are expected to become significant in the unpolluted and nighttime troposphere.[48] Formation of glycolaldehyde + CO + OH is expected to dominate, because of the smaller reaction barrier and the opportunity for significant quantum mechanical tunneling. Furthermore, because the critical barrier height is below that of the acrolein−OH adduct + O_2, it is possible that O_2 addition results in the formation of these new dissociated products in a direct chemically activated process.

Inner (α) OH Addition. Although OH addition to acrolein is known to predominantly take place at the outer β C atom, addition at the inner α carbon is also important and is considered in this study. An energy diagram for this process is shown in Figure 4, with optimized structures for $C_3H_5O_4$ minima and transition states provided in Figures 5 and 6, respectively.

From Figure 4 we observe that OH addition to the α carbon site in acrolein is considerably less exothermic than the β addition process, with a reaction enthalpy of around 28 kcal mol^{-1}. This likely explains the decreased barrier for OH addition to the unsaturated β versus α carbon. However, the peroxy radical that subsequently forms from O_2 addition at the α site has a similar enthalpy of formation to that produced in the β addition mechanism (cf. Table 1), as expected from group additivity arguments, and as a result association of the $C^{\bullet}H_2CH(OH)CHO$ radical with O_2 is around 34 kcal mol^{-1} exothermic. As such, this peroxy radical is provided with a considerable degree of excess vibrational energy that can go into further unimolecular isomerization and dissociation reactions prior to collisional deactivation. Three such low-energy reaction pathways are illustrated in Figure 4.

The $CH_2(OO^{\bullet})CH(OH)CHO$ radical can be considered to have β-hydroxyperoxy and β-formylperoxy functionalities and can also lose a methylene H atom to form a resonantly stabilized vinoxy-type radical. Intramolecular H atom abstraction from the hydroxy group proceeds via TSα1 with a barrier of 22.8 kcal mol^{-1} at the G3SX level, in a similar fashion to the corresponding reaction in the β OH addition mechanism. We also find that abstraction of the weak acyl H atom via the six-membered ring transition state TSα3, forming the $CH_2(OOH)CH(OH)C^{\bullet}O$ radical, requires a relatively small reaction barrier. At the G3SX level this barrier height is only 19.3 kcal mol^{-1}, or 14.6 kcal mol^{-1} below the acrolein−OH adduct + O_2 energy. Formation of $CH_2(OOH)CH(OH)C^{\bullet}O$ is again followed by CO loss, producing $CH_2(OOH)C^{\bullet}HOH$ (the further reactions of this species are discussed briefly below). A final process considered here is intramolecular C−H abstraction via TSα5, which forms the $CH_2(OOH)C^{\bullet}(OH)CHO$ radical. This radical is stabilized by resonance between the $CH_2(OOH)-C^{\bullet}(OH)-CH=O$ and

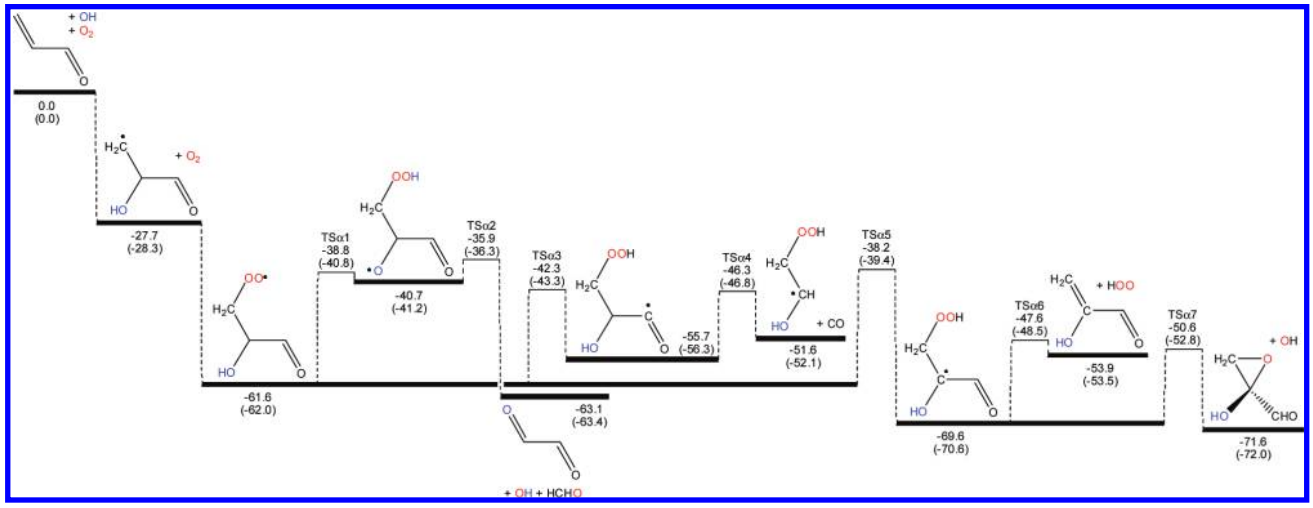

Figure 4. Energy surface for α OH addition to acrolein in air. Numbers are relative 298 K enthalpies with the G3SX (CBS-QB3) methods, in kcal mol^{-1}.

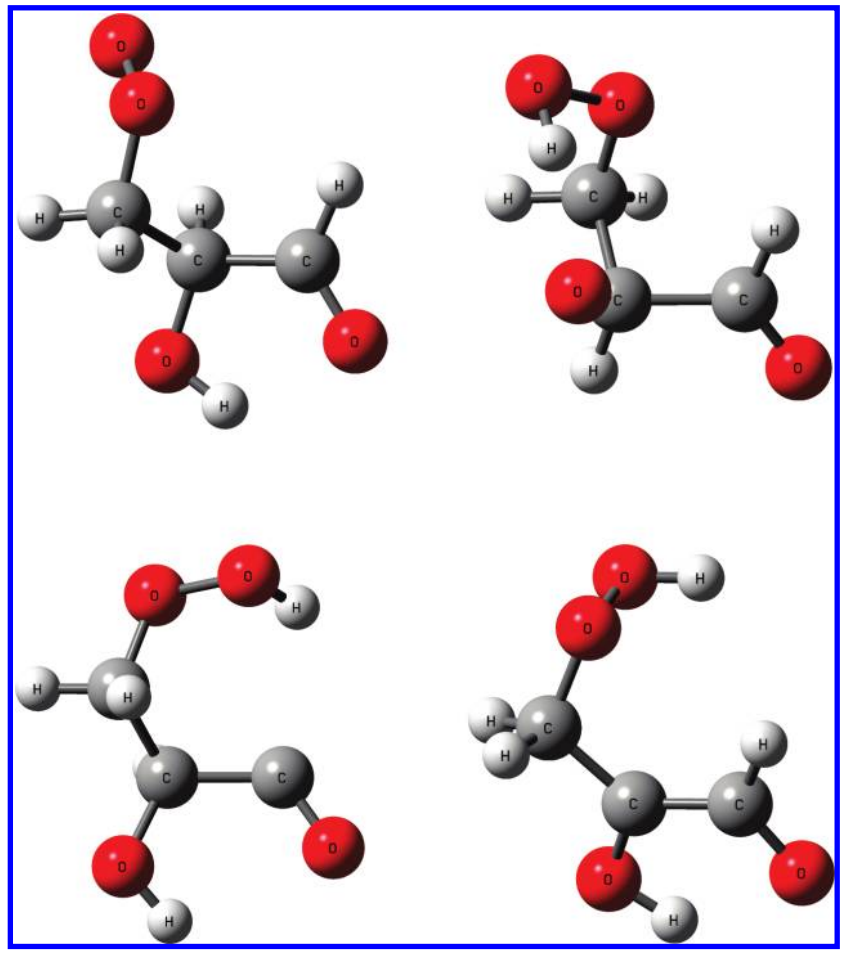

Figure 5. Optimized structures for $C_3H_5O_4$ minima arising from α OH addition to acrolein in air. Calculated at the B3LYP/6-31G(2df,p) level.

$CH_2(OOH)-C(OH)=CH-O^{\bullet}$ forms, making this reaction exothermic and with a relatively small barrier (23.4 kcal mol^{-1} at the G3SX level). Following this abstraction process, O atom attack on the radical site yields a functionalized epoxide plus OH, in a similar process to that recently identified in the reaction of isoprene hydroperoxides with OH.[50] In competition with this reaction, HO_2 elimination to form the enol $CH_2C(CHO)OH$ can also occur, but with a barrier that is 3.1 kcal mol^{-1} greater than that for formation of the epoxide, at the G3SX level.

This work demonstrates that the $CH_2(OO^{\bullet})CH(OH)CHO$ radical has several low-energy reaction pathways available to it, each proceeding at well below the initial energy of $C^{\bullet}H_2CH(OH)CHO$. Accordingly, it is likely that these product channels are accessed in the chemically activated reaction of $C^{\bullet}H_2CH(OH)CHO$ with O_2, even at ambient temperatures. The dominant reaction pathway is expected to be intramolecular H atom abstraction from the formyl group, yielding the $CH_2(OOH)C^{\bullet}HOH$ radical + CO. This radical should be able

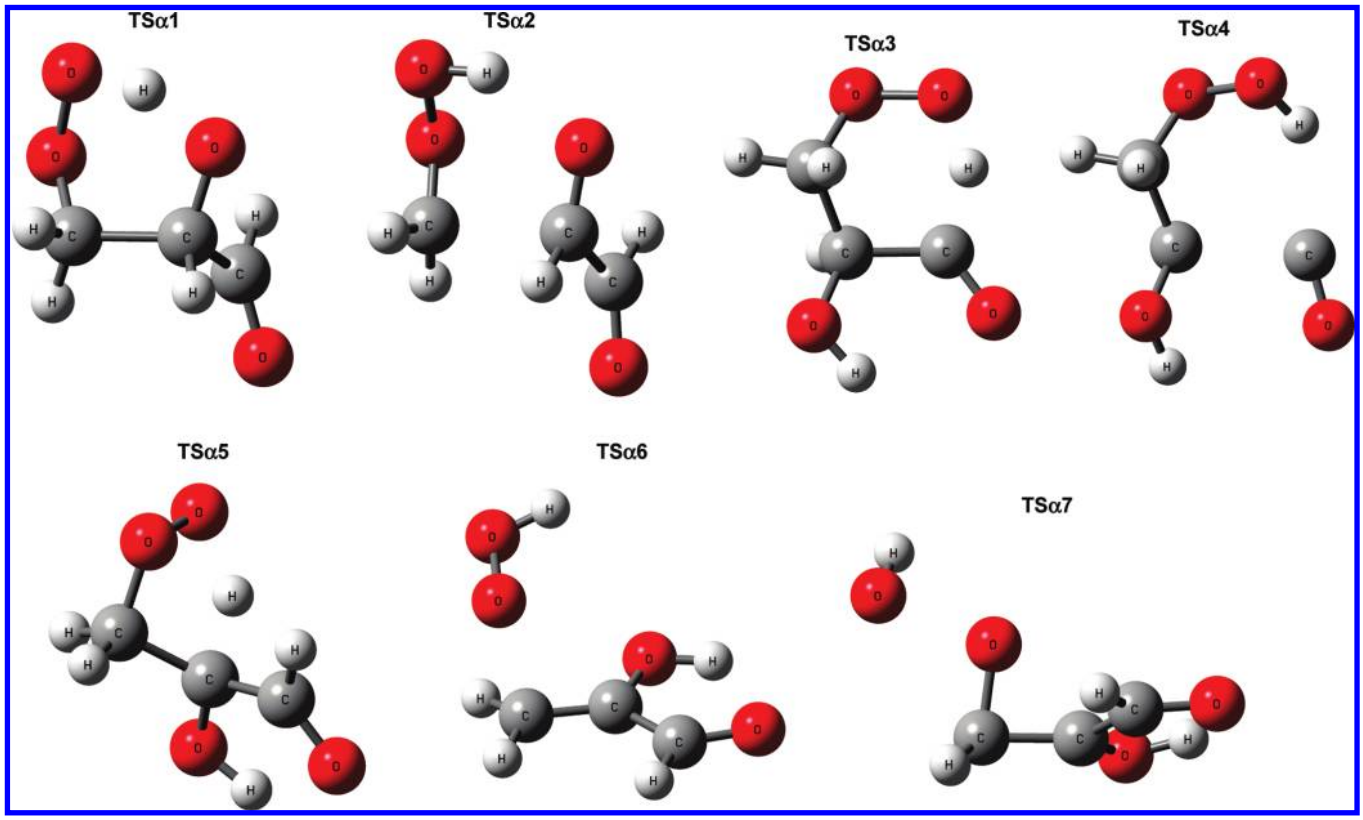

Figure 6. Optimized structures for $C_3H_5O_4$ transition states arising from α OH addition to acrolein in air. Calculated at the B3LYP/6-31G(2df,p) level.

to react with O_2 to form an α-hydroxyperoxy radical that readily eliminates HO_2, yielding $CH_2(OOH)CHO$.[51] Alternatively, since the $CH_2(OOH)C^{\bullet}HOH$ radical is expected to form with some excess vibrational energy, unimolecular reaction may compete with collisional deactivation/O_2 addition. We identify that this $CH_2(OOH)C^{\bullet}HOH$ radical eliminates OH to form the epoxide oxiranol, *c*-$CH_2OCH(OH)-$. At the G3SX level of theory, the barrier for this reaction is only 11.1 kcal mol^{-1}, which should make it accessible from even mildly activated $CH_2(OOH)C^{\bullet}HOH$, and therefore competitive with O_2 addition. This same OH elimination reaction has been previously proposed for the $CH_2(OOH)C^{\bullet}HOH$ radical formed in the $C^{\bullet}H_2CHOH + O_2$ reaction mechanism[51a] and is again a lower-energy process than HO_2 elimination to form the enol. Neither $CH_2(OOH)CHO$ or oxiranol appear to be experimentally detected acrolein oxidation products, although it is important to note that α OH addition is the least important process in the acrolein + OH reaction. Experimentally, exclusive formation of the $C^{\bullet}H_2CH(OH)CHO$ radical via photolysis of precursor molecules like $CH_2(I)CH(OH)CHO$ may be able to provide better resolution over the products of α OH addition to acrolein in air.

Importance to Tropospheric Chemistry. This study identifies several novel reaction pathways for the peroxy radicals formed following OH addition to acrolein in air, which proceed with energy at around or below that of the acrolein−OH adducts plus O_2. Furthermore, when secondary decomposition of the $CH_2(OOH)C^{\bullet}HOH$ radical is considered, these reactions all regenerate the OH radical used to initiate acrolein oxidation. Given low levels of NO and related radicals (ca. tens of ppt), thermal decomposition of the acrolein $C_3H_5O_4$ peroxy radicals is expected to compete with O atom abstraction. Furthermore, we propose here that activated $[C_3H_5O_4]^*$ adducts formed in the OH-initiated oxidation of acrolein can decompose in a formally direct process from association of O_2 with the activated [acrolein−OH]* adducts produced in the acrolein + OH addition reactions. Bimolecular reaction of vibrationally and electronically excited species, in competition with collisional deactivation, is not an unknown process. For example, competition between collisional deactivation of electronically excited $O(^1D)$ to a ground state oxygen atom by N_2 and O_2, and bimolecular reaction with less abundant molecules like H_2O, is the main source of photochemical OH in the atmosphere. Furthermore, direct OH production from the cyclohexyl radical + O_2 reaction, in a singly chemically activated process, has been observed to take place at even moderate temperature (ca. 600 K), high pressure (tens of atm) conditions.[52]

The addition of OH to acrolein is considerably exothermic, and in the atmosphere this process produces the vibrationally excited $[CH_2(OH)C^{\bullet}HCHO]^*$ and $[C^{\bullet}H_2CH(OH)CHO]^*$ radicals. These radicals will then be deactivated by collisions with N_2 and O_2 molecules, or react with O_2 to form the activated $[CH_2(OO^{\bullet})CH(OH)CHO]^*$ and $[CH_2(OO^{\bullet})CH(OH)CHO]^*$ peroxy radicals. If the acrolein−OH adducts carry even a relatively small amount of excess vibrational energy when O_2 addition occurs, the resultant peroxy radicals will have sufficient energy to access a range of decomposition channels, reforming OH with some non-negligible branching fraction. The two isomeric acrolein−OH radicals are expected to associate with O_2 with rate constants of around 10^{-11} cm^3 $molecule^{-1}$ s^{-1}, which is at near the collision limit; since these reactions are barrierless, these rate constants will also be relatively independent of temperature or [acrolein−OH]* radical energy. For an O_2 concentration of 5.1×10^{18} molecules cm^{-3} at 300 K and 1 atm, the acrolein−OH adduct lifetimes toward O_2 are predicted to be ca. 2×10^{-8} s. Given that a large fraction of [acrolein−OH]* collisions with O_2 are expected to result in reaction, and that a considerable

SCHEME 1: OH-Initiated Oxidation of MACR: β OH Addition

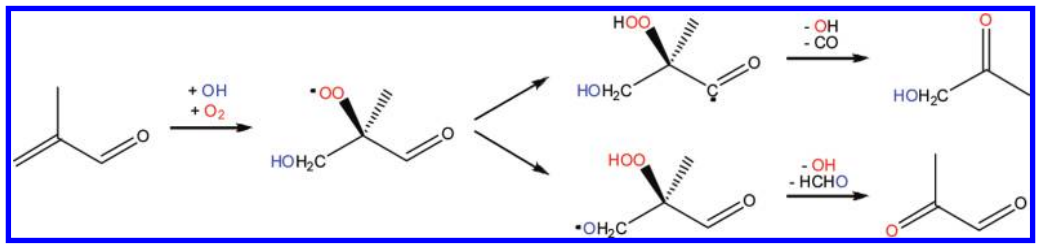

SCHEME 2: OH-Initiated Oxidation of MACR: α OH Addition

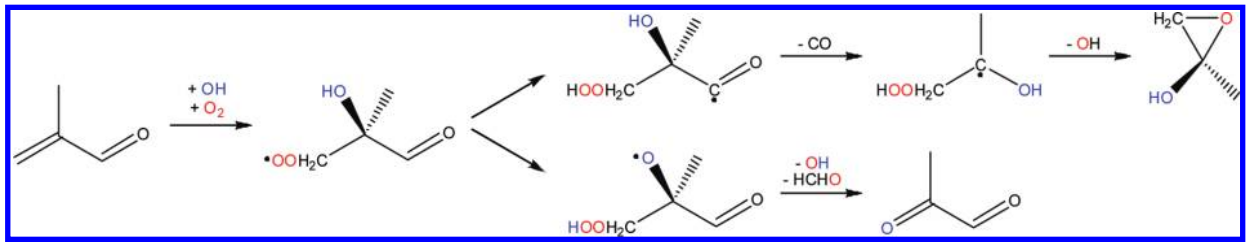

number of collisions with N_2 or O_2 will be required to deactivate these [acrolein−OH]* adducts (N_2 in particular is a poor collider, with each collision likely removing several kcal mol^{-1} or less of energy), it is expected that collisional deactivation takes place on a similar time scale to reaction with O_2. Double activation of the acrolein−OH-O_2 peroxy radicals would achieve prompt reformation of some fraction of OH, while also producing observed acrolein oxidation products such as glycolaldehyde + CO. Detailed experimental studies, along with chemical dynamics simulations, are needed to determine the potential importance of this double activation mechanism in the photochemical oxidation of acrolein and other related VOCs and OVOCs, although it is a viable process that, to our knowledge, is currently excluded from (O)VOC photochemical oxidation mechanisms.

As noted, acrolein is a model compound for both MACR and MVK, two of the most important OVOCs in the atmosphere. Several of the reaction pathways identified here are applicable to MACR and/or MVK, and warrant further exploration. The expected reaction scheme for β OH addition to MACR is shown in Scheme 1.

We see that β OH addition to MACR produces a peroxy radical that has the same pathways available to it as the analogous radical formed in acrolein oxidation. This MACR peroxy radical should be able to form hydroxyacetone ($CH_2(OH)C(O)CH_3$) + OH + CO, and to a lesser extent methylglyoxal + OH + HCHO, with relatively low barriers. Available products in the minor α OH addition channel for MACR are depicted below, where two of the three pathways for the corresponding process in acrolein are now available (Scheme 2). The above reaction scheme similarly provides a pathway to methylglyoxal + HCHO + OH as MACR oxidation products, with an alternative reaction that also reforms OH and produces a substituted epoxide.

The photochemical oxidation of MACR is known to proceed to a significant extent via OH addition at the outer carbon atom,[53] making reactions of the $CH_2(OH)C(CH_3)(OO^{\bullet})CHO$ radical of particular importance. We suggest that the OH-initiated oxidation of MACR has the ability to regenerate OH, and produce hydroxyacetone + CO, via peroxy radical decomposition and/or via a (doubly) chemically activated MACR−OH radical + O_2 reaction. Hydroxyacetone is a critical second-generation isoprene oxidation product that at present is not completely accounted for in atmospheric chemistry models.[54] Some evidence for reactions of this type has recently been reported, from Cl radical initiated oxidation of MACR.[55] Reaction of Cl with MACR in air predominantly proceeds via addition to the terminal carbon atom, where subsequent association with O_2 forms the $CH_2ClC(CH_3)(OO^{\bullet})CHO$ radical.[55] Further reaction of this peroxy radical with NO or other peroxy radicals in chamber experiments is thought to be responsible for formation of the major MACR + Cl oxidation product, chloroacetone ($CH_2ClC(O)CH_3$).[55,56] Strong evidence also exists for the formation of non-negligible quantities of OH radicals in the Cl-atom initiated oxidation of MACR,[55] which is not easily explained. By analogy to the processes studied here, OH radicals could be produced by unimolecular hydrogen transfer from the carbonyl group to the peroxy radical and subsequent decomposition (beta-scission) of $CH_2ClC(CH_3)(OOH)C^{\bullet}O$ to chloroacetone + CO. This could occur through the chemically activated reaction of $CH_2ClC^{\bullet}(CH_3)CHO$ with O_2, and by decomposition of the stabilized peroxy adduct.

The OH-initiated oxidation of MVK (Scheme 3) proceeds solely via an addition mechanism, due to the absence of a weak acyl H atom for abstraction. However, this also means that the low-energy intramolecular abstraction processes from the formyl group identified for acrolein will not be available in MVK oxidation. The potential oxidation pathways for MVK arising from this work are shown below, where the products are seen to be methylglyoxal + HCHO + OH. Again, formation of these products may take place via peroxy radical decomposition at low NO levels, or in chemically activated radical + O_2 reactions. It has also been suggested in the literature that rapid O_2 dissociation can be an important process in the unpolluted atmosphere,[46] and repeated cycling through O_2 addition/dissociation may be able to yield significant amounts of new, dissociated products (including OH) even if branching ratios to these chemically activated pathways are relatively low.[47,48]

The low-energy reactions identified here for the acrolein−OH-O_2 peroxy radicals are significant as they add to the growing pool of peroxy radicals that are expected to undergo unimolecular (versus bimolecular) reactions, and because they provide a new means for OH regeneration in the troposphere. The hydroxyl radical is the main agent for chemical destruction of compounds in the atmosphere, and OH levels therefore dictate the oxidative capacity of an air mass. In urban environments with large emissions of anthropogenic VOCs and nitrogen oxides (and resultant high ozone levels), elevated oxidative

SCHEME 3: OH-Initiated Oxidation of MVK

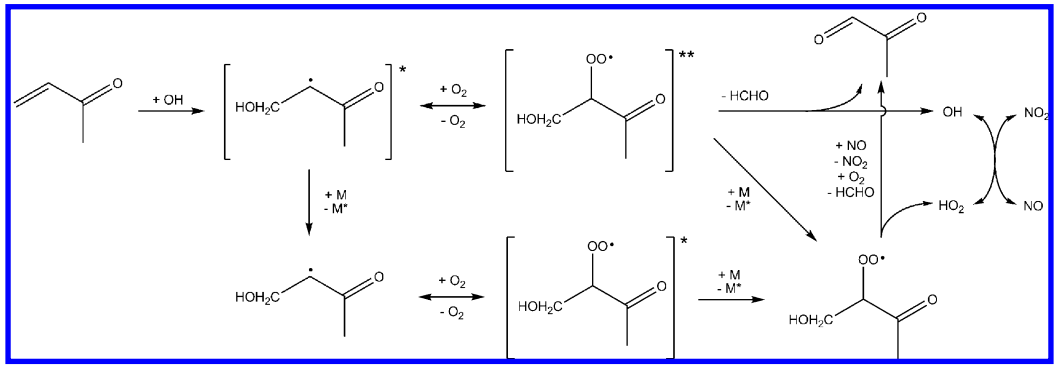

SCHEME 4: Conventional and Double Activation Reaction Processes

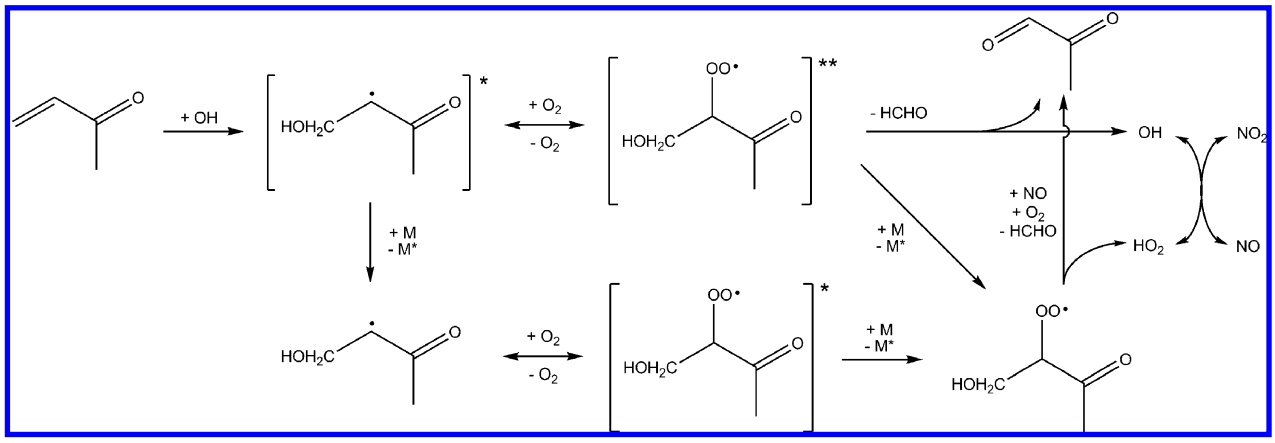

capacities are maintained by cycling between HO_2 and OH (HO_x) radicals, largely mediated by NO and O_3. In pristine environments such as the ocean boundary layer, low levels of NO_x and O_3 result in relatively low OH levels and high HO_2/OH ratios. A number of recent studies have indicated that in pristine forested environments with large sources of isoprene and other biogenic VOCs (particularly tropical rainforests), relatively high OH levels can be somehow maintained without the involvement of NO_x and O_3.[57,58] The reactions identified here for acrolein (particularly when extrapolated to MACR and MVK) may provide a new OH source in these pristine forested locations. Within this context the possibility of prompt OH reformation via a double activation mechanism is intriguing, as this process is independent of NO, and thus appears to result in no change between polluted and pristine environments. This is explored here for MVK, assuming that both the prompt OH-regenerating double activation mechanism and conventional peroxy radical formation (including subsequent reaction with NO) take place. In the presence of NO_x, the double activation mechanism is expected to proceed as

$$CH_2CHC(CH_3)O + OH (+ O_2) \rightarrow [CH_2(OH)CH(OO\bullet)C(CH_3)O]^{**} \rightarrow CH(O)C(CH_3)O + OH + HCHO$$
$$OH + NO_2 \leftrightarrow HO_2 + NO$$
$$CH_2CHC(CH_3)O + OH + O_2 + NO_2 \rightarrow CH(O)C(CH_3)O + HCHO + HO_2 + NO$$

The net result is for the conversion of MVK into two OVOCs (formaldehyde and methylglyoxal) in an HO_2-generating but HO_x-neutral process. Examining the conventional MVK oxidation process, with collisional deactivation of the $CH_2(OH)CH(OO^{\bullet})C(CH_3)O$ radical, the following reactions are expected (again, in the presence of NO_x):

$$CH_2CHC(CH_3)O + OH (+M) \rightarrow CH_2(OH)C\bullet HC(CH_3)O (+M)$$
$$CH_2(OH)C\bullet HC(CH_3)O + O_2 (+M) \rightarrow CH_2(OH)CH(OO\bullet)C(CH_3)O (+M)$$
$$CH_2(OH)CH(OO\bullet)C(CH_3)O + NO \rightarrow CH_2(OH)CH(O\bullet)C(CH_3)O + NO_2$$
$$CH_2(OH)CH(O\bullet)C(CH_3)O \rightarrow C\bullet H_2(OH) + CH(O)C(CH_3)O$$
$$C\bullet H_2(OH) \rightarrow HCHO + H$$
$$H + O_2 (+M) \rightarrow HO_2 (+M)$$
$$CH_2CHC(CH_3)O + OH + 2O_2 + NO \rightarrow CH(O)C(CH_3)O + HCHO + HO_2 + NO_2$$

Assuming that cycling between HO_x and NO_x radicals is efficient, the net result of this reaction scheme is the same as that of the double activation mechanism. This assumption is valid for polluted urban environments that rapidly achieve a steady-state between HO_x radicals. In the pristine troposphere, however, low NO and O_3 levels mean that this double activation mechanism could shift the HO_x balance from HO_2 to OH, as is observed in the field.[53] This is highlighted in Scheme 4, which incorporates both the conventional and double activation reaction processes. The main difference between the two mechanisms is the initial state of the HO_x radical that is produced. While this new chemistry may not fully account for the large OH source apparently missing from atmospheric chemistry models, it does add to the growing number of processes that can help to achieve this end. The potential for prompt OH recycling in the isoprene + OH reaction, via dissociation of activated β-hydroxyperoxy radicals,[46,47] is of particular interest.

Acknowledgment. Computational resources provided in part by the Victorian Partnership for Advanced Computing (VPAC).

Supporting Information Available: Optimized structures (B3LYP/6-31G(2df,p); G3SX and CBS-QB3 energies and enthalpies. This material is available free of charge via the Internet at http://pubs.acs.org.

References and Notes

(1) Berndt, T.; Böge, O. *J. Phys. Chem. A* **2007**, *111*, 12099.

(2) Liu, X.; Jefries, H. E.; Sexton, K. G. *Atmos. Environ.* **1999**, *33*, 3005.

(3) Tanimoto, H.; Akimoto, H. *Geophys. Res. Lett.* **2001**, *28*, 2831.

(4) Roberts, J. M.; Flocke, F.; Weinheimer, A.; Tanimoto, H.; Jobson, B. T.; Riemer, D.; Apel, E.; Atlas, E.; Donnelly, S.; Stroud, V.; Johnston, K.; Weaver, R.; Fehsenfeld, F. C. *Geophys. Res. Lett.* **2001**, *28*, 4195.

(5) Tuazon, E. C.; Alvarado, A.; Aschmann, S. M.; Atkinson, R.; Arey, J. *Environ. Sci. Technol.* **1999**, *33*, 3586.

(6) Pierotti, D.; Wofsy, S. C.; Jacob, D.; Rasmussen, R. A. *J. Geophys. Res.* **2004**, *95*, 1871.

(7) Montzka, S. A.; Trainer, M.; Goldan, D.; Kuster, W. C.; Fehsenfeld, F. C. *J. Geophys. Res.* **1993**, *98*, 1101.

(8) Warneke, C.; Holzinger, R.; Hansel, A.; Jordan, A.; Lindinger, W.; Pöschl, U.; Williams, J.; Hoor, P.; Fischer, H.; Crutzen, P. J.; Scheeren, H. A.; Lelieveld, J. *J. Atmos. Chem.* **2001**, *38*, 167.

(9) Poisson, N.; Kanakidou, M.; Crutzen, P. J. *J. Atmos. Chem.* **2000**, *36*, 157.

(10) Hori, M.; Matsunaga, N.; Marinov, N.; Pitz, W.; Westbrook, C. *Proc. Comb. Inst.* **1998**, *27*, 389.

(11) Dagaut, P.; Bakali, A. E.; Ristori, A. *Fuel* **2006**, *85*, 944.

(12) (a) Esterbauer, H.; Schaur, R. J.; Zollner, H. *Free Radical Biol. Med.* **1991**, *11*, 81. (b) Uchida, K.; Kanematsu, M.; Morimitsu, Y.; Osawa, T.; Noguchi, N. *J. Biol. Chem.* **1998**, *273*, 16058. (c) Uchida, K.; Kanematsu, M.; Sakai, K.; Matsuda, T.; Hattori, N.; Mizuno, Y.; Suzuki, D.; Miyata, T.; Noguchi, N.; Niki, E. *Proc. Natl. Acad. Sci. U.S.A.* **1998**, *95*, 4882. (d) Williams, T. I.; Lynn, B. C.; Markesbery, W. R.; Lovell, M. A. *Neurobiol. Aging* **2006**, *27*, 1094.

(13) Roden, P. J.; Stark, M. S.; Waddington, D. J. *Int. J. Chem. Kinet.* **1999**, *31*, 277.

(14) Orlando, J. J.; Tyndall, G. S. *J. Phys. Chem.* **2002**, *106*, 12252.

(15) Olivella, S.; Solé, A. *J. Chem. Theory Comput.* **2008**, *4*, 941.

(16) Vega-Rodriguez, A.; Alvarez-Idaboy, J. R. *Phys. Chem. Chem. Phys.* **2009**, *11*, 7649.

(17) El-Taher, S. *Can. J. Chem.* **2009**, *87*, 1716.

(18) (a) Nádasdi, R.; Szilágyi, I.; Zigner, G. L.; Dóbé, S.; Zádor, J.; Song, X.; Wang, B. Experimental and Theoretical Study of the Reactions $C_2H_5CO + O_2$ and $CH_3CHC(O)H + O_2$. In *Proc. 4th European Combust. Meeting*, Vienna, 2009. (b) da Silva, G.; Bozzelli, J. W. *J. Phys. Chem. A* **2006**, *110*, 13058. (c) Dóbé, S.; Khachatryan, L. A.; Bérces, T. *Ber. Bunsenges. Phys. Chem.* **1989**, *93*, 847. (d) Lansford, J. H. *Langmuir* **1989**, *5*, 12. (e) Nalbandyan, A. B.; Vardanyan, I. A. *Russ. Chem. Rev.* **1985**, *54*, 532.

(19) Asatryan, R.; Bozzelli, J. W. Oxidation of Acrolein by O_2 and OH Radicals. In *Proceedings, 6th US Combust. Meeting*, Ann Arbour, MI, USA, May 2009.

(20) Curtiss, L. A.; Redfern, P. C.; Raghavachari, K.; Pople, J. A. *J. Chem. Phys.* **2001**, *114*, 108.

(21) Montgomery, J. A., Jr.; Frisch, M. J.; Ochterski, J. W.; Petersson, G. A. *J. Chem. Phys.* **1999**, *110*, 2822.

(22) Frisch, M. J.; Trucks, G. W.; Schlegel, H. B.; Scuseria, G. E.; Robb, M. A.; Cheeseman, J. R.; Montgomery, Jr., J. A.; Vreven, T.; Kudin, K. N.; Burant, J. C.; Millam, J. M.; Iyengar, S. S.; Tomasi, J.; Barone, V.; Mennucci, B.; Cossi, M.; Scalmani, G.; Rega, N.; Petersson, G. A.; Nakatsuji, H.; Hada, M.; Ehara, M.; Toyota, K.; Fukuda, R.; Hasegawa, J.; Ishida, M.; Nakajima, T.; Honda, Y.; Kitao, O.; Nakai, H.; Klene, M.; Li, X.; Knox, J. E.; Hratchian, H. P.; Cross, J. B.; Adamo, C.; Jaramillo, J.; Gomperts, R.; Stratmann, R. E.; Yazyev, O.; Austin, A. J.; Cammi, R.; Pomelli, C.; Ochterski, J. W.; Ayala, P. Y.; Morokuma, K.; Voth, G. A.; Salvador, P.; Dannenberg, J. J.; Zakrzewski, V. G.; Dapprich, S.; Daniels, A. D.; Strain, M. C.; Farkas, O.; Malick, D. K.; Rabuck, A. D.; Raghavachari, K.; Foresman, J. B.; Ortiz, J. V.; Cui, Q.; Baboul, A. G.; Clifford, S.; Cioslowski, J.; Stefanov, B. B.; Liu, G.; Liashenko, A.; Piskorz, P.; Komaromi, I.; Martin, R. L.; Fox, D. J.; Keith, T.; Al-Laham, M. A.; Peng, C. Y.; Nanayakkara, A.; Challacombe, M.; Gill, P. M. W.; Johnson, B.; Chen, W.; Wong, M. W.; Gonzalez, C.; and Pople, J. A. *Gaussian 03, Revision D.01*; Gaussian, Inc.: Wallingford CT, 2004.

(23) Frisch, M. J.; Trucks, G. W.; Schlegel, H. B.; Scuseria, G. E.; Robb, M. A.; Cheeseman, J. R.; Montgomery, Jr., J. A.; Vreven, T.; Kudin, K. N.; Burant, J. C.; Millam, J. M.; Iyengar, S. S.; Tomasi, J.; Barone, V.; Mennucci, B.; Cossi, M.; Scalmani, G.; Rega, N.; Petersson, G. A.; Nakatsuji, H.; Hada, M.; Ehara, M.; Toyota, K.; Fukuda, R.; Hasegawa, J.; Ishida, M.; Nakajima, T.; Honda, Y.; Kitao, O.; Nakai, H.; Klene, M.; Li, X.; Knox, J. E.; Hratchian, H. P.; Cross, J. B.; Bakken, V.; Adamo, C.; Jaramillo, J.; Gomperts, R.; Stratmann, R. E.; Yazyev, O.; Austin, A. J.; Cammi, R.; Pomelli, C.; Ochterski, J. W.; Ayala, P. Y.; Morokuma, K.; Voth, G. A.; Salvador, P.; Dannenberg, J. J.; Zakrzewski, V. G.; Dapprich, S.; Daniels, A. D.; Strain, M. C.; Farkas, O.; Malick, D. K.; Rabuck, A. D.; Raghavachari, K.; Foresman, J. B.; Ortiz, J. V.; Cui, Q.; Baboul, A. G.; Clifford, S.; Cioslowski, J.; Stefanov, B. B.; Liu, G.; Liashenko, A.; Piskorz, P.; Komaromi, I.; Martin, R. L.; Fox, D. J.; Keith, T.; Al-Laham, M. A.; Peng, C. Y.; Nanayakkara, A.; Challacombe, M.; Gill, P. M. W.; Johnson, B.; Chen, W.; Wong, M. W.; Gonzalez, C.; and Pople, J. A. *Gaussian 09, Revision A.02*; Gaussian, Inc.: Wallingford CT, 2009.

(24) Zheng, J.; Zhao, Y.; Truhlar, D. G. *J. Chem. Theory Comput.* **2009**, *5*, 808.

(25) da Silva, G.; Moore, E. E.; Bozzelli, J. W. *J. Phys. Chem. A* **2009**, *113*, 10264.

(26) Recommended in ref 27 based upon previous calculations in ref 28. No experimental value for this property could be located.

(27) Li, Y.; Baer, T. *Int. J. Mass Spectrom.* **2002**, *218*, 37.

(28) (a) Allinger, N. L.; Rodriguez, S.; Chen, K. *J. Mol. Struct. THEOCHEM* **1992**, *260*, 161. (b) McKee, M. L.; Radom, L. *Org. Mass Spectrom.* **1993**, *28*, 1238. (c) Li, Y.; Baer, T. *Int. J. Mass Spectrom.* **2002**, *218*, 19.

(29) Ruscic, B.; Wagner, A. F.; Harding, L. B.; Asher, R. L.; Feller, D.; Dixon, D. A.; Peterson, K. A.; Song, Y.; Qian, X.; Ng, C.-Y.; Liu, J.; Chen, W.; Scwenke, D. W. *J. Phys. Chem. A* **2002**, *106*, 2727.

(30) (a) Fletcher, R. A.; Pilcher, G. *Trans. Faraday Soc.* **1970**, *66*, 794. (b) Dorofeeva, O.; Novikov, V. P.; Neumann, D. B. *J. Phys. Chem. Ref. Data* **2001**, *30*, 475.

(31) da Silva, G.; Bozzelli, J. W.; Sebbar, N.; Bockhorn, H. *ChemPhysChem* **2006**, *7*, 1119.

(32) Theoretical value of: Espinosa-Garcia, J.; Dobe, S. *J. Mol. Struct. THEOCHEM* **2005**, *713*, 119.

(33) Cox, J. D.; Wagman, D. D.; Medvedev, V. A. *CODATA Key Values for Thermodynamics*; Hemisphere Pubishing Corp.: New York, 1984.

(34) Ruscic, B.; Pinzon, M. L.; Morton, M. L.; Srinivasan, N. K.; Su, M.-C.; Sutherland, J. W.; Michael, J. V. *J. Phys. Chem. A* **2006**, *110*, 6592.

(35) da Silva, G.; Bozzelli, J. W.; Asatryan, R. *J. Phys. Chem. A* **2009**, *113*, 8596.

(36) Alfassi, Z. B.; Golden, D. M. *J. Am. Chem. Soc.* **1973**, *95*, 1973.

(37) Anderson, E. A.; Hood, G. C. Physical Properties. In: *Acrolein*; Smith, C. E., Ed.; Wiley: New York, 1962.

(38) Lias, S. G.; Bartmess, J. E.; Liebman, J. F.; Holmes, J. L.; Levin, R. D.; Mallard, W. G. *J. Phys. Chem. Ref. Data Supp. 1* **1988**, *17*, 1.

(39) Vajda, J. H.; Harrison, A. G. *Int. J. Mass Spectrom. Ion Phys.* **1979**, *30*, 293.

(40) Sebbar, N.; Bozzelli, J. W.; Bockhorn, H. *Int. J. Chem. Kinet.* **2005**, *37*, 633.

(41) Sebbar, N.; Bockhorn, H.; Bozzelli, J. W. *J. Phys. Chem. A* **2005**, *109*, 2233.

(42) Kondo, S.; Takahashi, A.; Tokuhashi, K. *J. Haz. Mat.* **2002**, *A94*, 37.

(43) Morales, G.; Martinez, R. *J. Phys. Chem. A* **2009**, *113*, 8683.

(44) Martin, J. M. L.; de Oliveira, G. *J. Chem. Phys.* **1999**, *111*, 1843.

(45) (a) MultiWell-2010.1 Software, 2010, designed and maintained by John R. Barker with contributors Ortiz, N. F.; Preses, J. M.; Lohr, L.; Maranzana, A.; Stimac, P. J.; Lam, N. T.; Dhilip Kumar, T. J. University of Michigan, Ann Arbor, MI; http://aoss.engin.umich.edu/multiwell/. (b) Nguyen, T. L.; Barker, J. R. *J. Phys. Chem. A* **2010**, *114*, 3718.

(46) Peeters, J.; Nguyen, T. L.; Vereecken, L. *Phys. Chem. Chem. Phys.* **2009**, *11*, 5935–5939.

(47) da Silva, G.; Graham, C.; Wang, Z.-F. *Environ. Sci. Technol.* **2010**, *44*, 250.

(48) da Silva, G. *J. Phys. Chem. A* **2010**, *114*, 6861.

(49) da Silva, G. *Phys. Chem. Chem. Phys.* **2010**, *12*, 6698.

(50) Paulot, F.; Crounse, J. D.; Kjaergaard, H. G.; Kurten, A.; St. Clair, J. M.; Seinfeld, J. H.; Wennberg, P. O. *Science* **2009**, *325*, 730.

(51) (a) Zador, J.; Fernandes, R. X.; Georgievskii, Y.; Meloni, G.; Taatjes, C. A.; Miller, J. A. *Proc. Combust. Inst.* **2009**, *32*, 271. (b) da Silva, G.; Bozzelli, J. W.; Liang, L.; Farrell, J. T. *J. Phys. Chem. A* **2009**, *113*, 8923.

(52) Fernandes, R. X.; Zador, J.; Jusinski, L. E.; Miller, J. A.; Taatjes, C. A. *Phys. Chem. Chem. Phys.* **2009**, *11*, 1320.

(53) (a) Tuazon, E. C.; Atkinson, R. *Int. J. Chem. Kinet.* **1990**, *22*, 591. (b) Orlando, J. J.; Tyndall, G. S.; Paulson, S. E. *J. Geophys. Res.* **1999**, *26*, 2191.

(54) Karl, T.; Guenther, A.; Turnipseed, A.; Tyndall, G.; Artaxo, P.; Martin, S. *Atmos. Chem. Phys.* **2009**, *9*, 7753.

(55) Kaiser, E. W.; Pala, I. R.; Wallington, T. J. *J. Phys. Chem. A* **2010**, *114*, 6850.

(56) (a) Canosa-Mas, C. E.; Cotter, E. S. N.; Duffy, J.; Thompson, K. C.; Wayne, R. P. *Phys. Chem. Chem. Phys.* **2001**, *3*, 3075. (b) Orlando, J. J.; Tyndall, G. S.; Apel, E. C.; Riemer, D. D.; Paulson, S. E. *Int. J. Chem. Kinet.* **2003**, *35*, 335.

(57) Lelieveld, J.; Butler, T. M.; Crowley, J. N.; Dillon, T. J.; Fischer, H.; Ganzeveld, L.; Harder, H.; Lawrence, M. G.; Martinez, M.; Taraborrelli, D.; Williams, J. *Nature* **2008**, *452*, 737.

(58) Hofzumahaus, A.; Rohrer, F.; Lu, K.; Bohn, B.; Brauers, T.; Chang, C.-C.; Fuchs, H.; Holland, F.; Kita, K.; Kondo, Y.; Li, X.; Lou, S.; Shao, M.; Zeng, L.; Wahner, A.; Zhang, Y. *Science* **2009**, *324*, 1702.

JP104828A